ORIGINAL ARTICLE

Cancer Science WILEY

Luteolin suppresses bladder cancer growth via regulation of mechanistic target of rapamycin pathway

Keitaro Iida[1,2] | Taku Naiki[1,2] iD | Aya Naiki-Ito[1] iD | Shugo Suzuki[1] iD |
Hiroyuki Kato[1] | Satoshi Nozaki[2] | Takashi Nagai[2] | Toshiki Etani[2] | Yuko Nagayasu[1] |
Ryosuke Ando[2] | Noriyasu Kawai[2] | Takahiro Yasui[2] iD | Satoru Takahashi[1] iD

[1]Department of Experimental Pathology and Tumor Biology, Nagoya City University Graduate School of Medical Sciences, Nagoya, Japan

[2]Department of Nephro-Urology, Nagoya City University Graduate School of Medical Sciences, Nagoya, Japan

Correspondence
Aya Naiki-Ito, Department of Experimental Pathology and Tumor Biology, Nagoya City University Graduate School of Medical Sciences, 1-Kawasumi, Mizuho-cho, Mizuho-ku 467-8601, Nagoya, Japan.
Email: ayaito@med.nagoya-cu.ac.jp

Funding information
TOBE MAKI Scholarship Foundation, Grant/Award Number: 18-JA-501; Aichi Health Promotion Fundation, Grant/Award Number: 30127; Ministry of Health, Labour and Welfare, Grant/Award Number: 18K16705

Abstract

Luteolin is a natural flavonoid with strong anti–oxidative properties that is reported to have an anti–cancer effect in several malignancies other than bladder cancer. In this study, we describe the effect of luteolin on a human bladder cancer cell line, T24, in the context of the regulation of p21, thioredoxin-1 (TRX1) and the mechanistic target of rapamycin (mTOR) pathway. Luteolin inhibited cell survival and induced G2/M cell-cycle arrest, p21 upregulation and downregulation of phospho(p)-S6, which is downstream of mTOR signaling. Luteolin also upregulated TRX1 and reduced intracellular reactive oxygen species production. In a subcutaneous xenograft mouse model using the rat bladder cancer cell line, BC31, tumor volumes were significantly decreased in mice orally administered luteolin compared to control. Immunohistochemical analysis revealed that increased p21 and decreased p-S6 expression were induced in the luteolin treatment group. Moreover, in another in vivo N-butyl-N-(4-hydroxybutyl) nitrosamine (BBN)-induced rat bladder cancer model, the oral administration of luteolin led to a trend of decreased bladder tumor dimension and significantly decreased the Ki67-labeling index and p-S6 expression. Furthermore, the major findings on the metabolism of luteolin suggest that both plasma and urine luteolin-3'-O-glucuronide concentrations are strongly associated with the inhibition of cell proliferation and mTOR signaling. Moreover, a significant decrease in the squamous differentiation of bladder cancer is attributed to plasma luteolin-3'-glucuronide concentration. In conclusion, luteolin, and in particular its metabolized product, may represent another natural product-derived therapeutic agent that acts against bladder cancer by up-regulating p21 and inhibiting mTOR signaling.

KEYWORDS

animal model, bladder cancer, chemoprevention, mTOR, oxidative stress

1 | INTRODUCTION

Bladder cancer is the tenth most common cancer in the world, with an estimated 549 000 new cases and 200 000 deaths annually.[1] Approximately 75% of bladder cancer patients are diagnosed with non–muscle-invasive bladder cancer (NMIBC); however, the remaining 25% have muscle-invasive bladder cancer (MIBC) or metastatic disease at the time of initial diagnosis. More than half of patients with NMIBC have disease recurrence and 10%-15% develop disease progression. Chemotherapy and immuno-oncology drugs can be partially effective against recurrence and metastasis of MIBC after cystectomy; however, overall survival is still less than a year.[2] Therefore, alternative or supportive treatments for bladder cancer are needed.

Oxidative stress arises from an imbalance between reactive oxygen species (ROS) production and redox systems. It can indicate carcinogenesis and promote cell proliferation in various organs. Smoking is the greatest risk factor for death from bladder cancer as well as its incidence.[1,3] Excessive ROS production in response to cigarette smoke acts as an oxidative stress that can induce genomic instability and promote tumorigenesis.[4,5]

Flavonoids are polyphenolic compounds found in fruits or vegetables that are believed to provide a health benefit. Luteolin, a flavonoid found in perilla, parsley and green peppers, scavenges ROS.[6] Luteolin shows an anti–cancer effect in a variety of cancers, including colon, pancreatic, prostate and lung cancer, and has anti–oxidative, anti–inflammatory and anti–allergic properties.[6,7] We have previously found that luteolin has a preventive role in non–alcoholic steatohepatitis-related hepatocarcinogenesis through suppression of hepatic ROS accumulation and NF-κB signaling.[8] However, the anti–cancer effect of luteolin in bladder cancer has received little attention in the literature.

Thioredoxin-1 (TRX1) is 12-kDa thiol redox-active protein that is believed to protect individuals from oxidative stress-induced damage by scavenging ROS. TRX1 is translocated into the nucleus to regulate the activity of transcription factors such as activator protein-1, NF-κB and p53, and plays an important role in the regulation of cell viability and activation.[9-11] An elevated level of TRX1 is found in various human cancers, such as lung, liver, colorectal and prostate cancers, as compared to their respective normal tissues.[11,12] In addition, enhanced TRX1 levels are often reported in many types of cancers that have progressed, metastasized or become resistant to chemotherapy.[9,10] For instance, castration-resistant prostate cancer cells showed enhanced TRX1 expression under androgen-deprived conditions.[11] Elevated TRX1 expression may be the consequence of accumulated ROS generated by cancer cells after exposure to antineoplastic agents.[5,13] However, TRX1 itself may not always have oncogenic functions.[11] To date, the role of TRX1 expression in bladder cancer remains to be elucidated.

The mechanistic target of rapamycin (mTOR), a highly conserved serine–threonine kinase, acts as an anti–cancer agent to inhibit cellular growth or proliferation as well as an immunosuppressant in several cancers, including bladder cancer cells.[14-16] The intraperitoneal administration of an mTOR inhibitor reduced the proliferation and tumor incidence of bladder cancer in an N-butyl-N-(4-hydroxybutyl) nitrosamine (BBN)-induced mouse bladder cancer model.[16] A single treatment with an mTOR inhibitor, everolimus, in patients with metastatic urothelial carcinoma (UC) resulted in a 31% objective response rate (ORR), in the form of tumor regression, including a near-complete response and a partial response.[17] Moreover, another phase II study of dual treatment with phosphoinositol-3-kinase and mTOR inhibitors in locally advanced or metastatic patients with UC demonstrated that the ORR was 15%, with 50% of patients experiencing grade 3-4 adverse events.[18] These studies indicate that mTOR inhibition has the potential to suppress bladder cancer, although the benefit is not as strong as expected.

The relationships among oxidative stress, TRX1 and the mTOR pathway have been outlined in previous studies. Cysteine oxidants, having an opposing function to anti–oxidants, stimulate mTOR complex 1 (mTORC1) activity via Rheb.[19] British anti–lewisite, which can reverse oxidation reactions, strengthened the interaction between mTORC1 and raptor, and inhibited ribosomal protein S6 kinase1 (S6K1) phosphorylation.[20] Furthermore, TRX1 had a protective role in cardiomyocytes by interacting directly with mTOR.[21]

In this study, we describe an anti–proliferative effect of luteolin in human bladder cancer cell lines. We also describe a suppressive effect of dietary luteolin in rat bladder cancer tumor and BBN-induced bladder carcinogenesis models. The inhibitory effect of luteolin was due to p21 upregulation and decreased phospho(p)-S6, which is a substrate of mTORC1. Furthermore, we identified a metabolite of luteolin in plasma and urine that strongly contributed to its chemopreventive activity.

2 | MATERIALS AND METHODS

2.1 | Cell culture and reagents

The human bladder cancer cell lines, T24, 5637 with a *p53* mutation and RT-4 with wild-type *p53*, were acquired from the ATCC and maintained in DMEM and RPMI 1640, respectively (Thermo Fisher Scientific), supplemented with 10% FBS. All cells were authenticated by DNA profiling using short tandem repeat analysis. A rat bladder cancer cell line, BC31 with a *p53* mutation, was derived from a BBN-induced rat bladder cancer and cultured as previously described.[22-24] All cells were cultured at 37°C in a humidified atmosphere of 5% CO_2. Luteolin (3,4,5,7-tetrahydroxy flavone) and 1-methylpropyl 2-imidazolyl disulfide (PX-12) were purchased from Tokyo Chemical Industry and Sigma–Aldrich, respectively.

2.2 | Cell viability assay

T24 and 5637 cells were seeded in 96-well plates at a density of 3×10^3 cells/well. The cells were grown for 24 hours and treated with luteolin for 48 hours. Cell viability was evaluated using Cell

Counting Kit-8 (Dojindo Laboratories). All experiments were performed in triplicate.

2.3 | Flow cytometry of apoptosis and cell-cycle analysis

Cells were treated with luteolin for 48 hours and collected in 6-well plates. A FACSCalibur system (BD) was used for both apoptosis and cell-cycle assays. We used a phycoerythrin Annexin V Apoptosis Detection Kit with 7-aminoactinomycin D (BioLegend) for apoptosis assays, and a Cell Cycle Phase Detection Kit (Cayman Chemical) to evaluate the cell cycle by propidium iodide according to the manufacturer's instructions. All experiments were performed in triplicate.

2.4 | Western blot analysis

All proteins were collected from cells at 70%-80% confluency in 6-well plates. A total of 30 μg protein per lane was resolved on 12% acrylamide gels and transferred onto Hybond ECL membranes (GE Healthcare UK). Primary antibodies and their dilution ratios are listed in Table S1. All experiments were performed in triplicate.

2.5 | In vitro *siRNA* transfection

Small interfering (si)RNAs targeting human *TP53* sequences were obtained from Sigma-Aldrich. RT4 cells (1.5×10^5/well) were seeded in 6-well plates and transfected with 20 nmol/L siRNA using Lipofectamine RNAiMAX (Thermo Fischer Scientific) according to the manufacturer's protocol.[8] Non–targeting siRNA, with no significant homology to any known rat and human genes, was also used as a negative control (NC). Confirmation of *TP53* knockdown and treatment with luteolin were performed 24 hours after transfection. All experiments were performed in triplicate.

2.6 | TRX1 gene expression analysis

The Cancer Genome Atlas (TCGA) bladder cancer datasets (http://cancergenome.nih.gov/) were analyzed as previously described.[11] The unit is Fragments Per Kilobase of transcript per Million mapped reads Upper Quartile (FPKM-UQ).

2.7 | TRX1 and DCFH-DA assay

TRX1 levels were evaluated using a Human Thioredoxin Assay Kit (IBL). Briefly, T24 cells were seeded into 6-well plates followed by a 48-hour exposure to luteolin. After treating the medium of each plate according to the manufacturer's instructions, we measured absorbance at 450 nm using a microplate reader. A dichloro-dihydro-fluorescein diacetate (DCFH-DA) assay was performed to evaluate intracellular ROS production, as previously described.[22] All experiments were performed in triplicate.

2.8 | Cancer patient tissue samples

A total of 166 patients who underwent radical cystectomy or transurethral resection for bladder cancer and whose pathology was UC or its variants, as diagnosed by experienced pathologists, were eligible for this study. This study was approved by the institutional review board at Nagoya City University Hospital and the approval number was NCU-893. All enrolled patients provided written informed consent.

2.9 | Animals

Three or four experimental rats or mice were housed in each plastic cage on wood-chip bedding in an air-conditioned specific pathogen-free animal room at 22 ± 2°C and 55% ± 5% humidity with a 12-hour light/dark cycle. Food and tap water were available ad libitum. The present experiments were performed under protocols approved by the Institutional Animal Care and Use Committee of Nagoya City University School of Medical Sciences.

2.10 | Xenograft mouse model

Seven-week-old male KSN nude mice (Japan SLC) were inoculated subcutaneously in the back with 5×10^4 BC31 cells. Two days after injection, 24 mice were randomly divided into two treatment groups and fed either an AIN76A control diet (Oriental Bio Science) or AIN76A with 100 ppm luteolin for 5 weeks. Tumor size was monitored weekly. Tumor volume was calculated using the following formula: 1/2 × Length ×Width × Height.

2.11 | N-butyl-N-(4-hydroxybutyl) nitrosamine-induced rat bladder carcinogenesis model

Six-week-old male F344 rats (Charles River Laboratories Japan) were given 0.05% BBN (Tokyo Chemical Industry) in drinking water for 10 weeks. A total of 60 rats were then randomly divided into three groups and received either a control diet, or 20 or 100 ppm luteolin for 20 weeks. A 24-hour specimen of urine was collected in the 29th week. All rats were killed, and blood, bladders, livers and kidneys were collected in the 30th week. Bladder tissues were divided equally into four portions and fixed by formalin, and H&E stains of all specimens were evaluated by experienced pathologists (N.A-I, SS) according to previously described instructions.[25] Each tumor dimension was quantified using a BZ-9000 multifunctional microscope and associated analysis software (Keyence).

2.12 | DNA extraction and direct sequencing for p53 gene in N-butyl-N-(4-hydroxybutyl) nitrosamine-induced rat bladder cancers

Genomic DNA was extracted from BBN-induced rat bladder tumors histologically diagnosed as cancer from the control group (n = 10) and the luteolin 100 ppm group (n = 10). The extraction from formalin-fixed paraffin-embedded tissues was performed using NucleoSpin DNA FFPEXS (MACHEREY-NAGEL). Exons 5, 6-7 and 8 of rat *p53* gene were analyzed as previously reported.[26] The primer sequences were 5′-CGCTGACCTTTGATTCTTTC-3′ and 5′-AGTTCTAACCC CACAGCAGT-3′ for exon 5, 5′-GTTAGAACTGGTTGTCCAGGG-3′ and 5′-CCCAACCTGGCACACAGCTTCCT-3′ for exon 6-7, and 5′-CTGTGC TCCTCTTGTCCCG-3′ and 5′-CCTCCACCTTCTTTGTCCTG-3′ for exon 8. PCR products were purified with NucleoSpin Gel and PCR Clean-up (MACHEREY-NAGEL). Direct sequencing was performed using 2 μL of aliquots by Applied Biosystems 3130xl Genetic Analyzer (Thermo Fischer Scientific) according to the manufacture's instructions. Sequencing primers for exon 5 were 5′-GATTCTTTCTCCTCTCCTACAG-3′ and 5′-AGTTCTAACCCCACA GCAGT-3′, for exon 6-7 were 5′-GCCTCTGACTTATTCTTGCT-3′ and 5′-AACCTGGCACACAGCTTCCT-3′, and for exon 8 were 5′-TGCCTCC TCTTGTCCCGGGT-3′ and 5′-CACCTTCTTTGTCCTGCCTG-3′.

2.13 | Immunohistochemistry and histological analysis

Deparaffinized formalin-fixed human and rat tissues were incubated with primary antibodies (listed in Table S2). A TUNEL assay was performed using an In situ Apoptosis Detection Kit from Takara, as previously described.[22] Immunostaining was done according to the manufacturer's instructions.[27]

In the analysis of positive cell rates for Ki67, TUNEL and p21, five microscopic fields were randomly selected and quantified with the same threshold nuclear intensity at a ×400 magnification according to analysis software (Keyence). The cytoplasmic intensities of p-S6 and cytokeratin 5/6 (CK5/6) were randomly selected in five cancerous areas at ×400 magnification and quantified with analysis software.

2.14 | Metabolism of luteolin

Plasma and urine luteolin levels in F344 rats (control: n = 10, luteolin 100 ppm: n = 18) were analyzed by HPLC-tandem mass spectrometry at the Biodynamic Plant Institute. All samples were analyzed using the API 3200 System (ABSciex) with an HPLC system (Shimazu, Kyoto, Japan). Chromatographic separation was achieved on a YMC-Pack ProC18 (5 μm, 3.0 mm × 150 mm; YMC) and maintained at 40°C at a flow rate of 0.3 mL/min. The concentrations of luteolin-aglycone, luteolin-7-glucoside and luteolin-3′-glucuronide were measured.

2.15 | Statistical analysis

Data were analyzed using EZR software (Saitama Medical Center, Jichi Medical University) and Fisher's exact test, Student's *t* test or ANOVA, where appropriate. Spearman's rank correlation coefficient was used to evaluate the correlation of two variables. $P < 0.05$ was considered a statistically significant difference.

3 | RESULTS

3.1 | Luteolin has a cancer suppressive effect and upregulates p21$^{Waf1/Cip1}$ in bladder cancer cells

As shown in Figure 1A, luteolin had an inhibitory effect on the cell viability in a dose-dependent manner against human bladder cancer cell lines. Figure 1B,C and Figure S1A show that luteolin clearly induced apoptosis in bladder cancer cells. Next, we found that luteolin induced G2/M arrest in a dose-dependent manner (Figure 1D,1 and Figure S1B). We further explored changes in cell-cycle-related protein expression in response to treatment with luteolin. We found upregulated p21$^{Waf1/Cip1}$ and p27^{Kip1}, and downregulated cyclin A and D1 in luteolin-treated T24 cells, which were derived from a high-grade human bladder cancer (Figure 1F). The upregulated expression of p21$^{Waf1/Cip1}$ and decreased expression of cyclin D1 with luteolin treatment were also evident in a low-grade human bladder cancer cell line, 5637 (Figure 1F). To explore the effect of p53 function on p21$^{Waf1/Cip1}$ regulation by luteolin, we further demonstrated an effect on a p53 wild-type human bladder cancer cell line, RT4. The expression level of p21$^{Waf1/Cip1}$ was higher in RT4 cells compared to T24 and 5637 cells. Luteolin increased the expression of p21$^{Waf1/Cip1}$ in RT4 cells (Figure 1G). *TP53* knockdown clearly downregulated p21$^{Waf1/Cip1}$, indicating that p21$^{Waf1/Cip1}$ expression was p53-dependent. Luteolin still upregulated p21$^{Waf1/Cip1}$ in *TP53*-silenced RT4 cells (Figure 1H). Taken together, luteolin induces p21$^{Waf1/Cip1}$ in bladder cancer cells with both *p53* wild-type and mutation.

FIGURE 1 Luteolin has a cancer suppressive effect and upregulates p21Waf1/Cip1 in human bladder cancer cells. A, Cell viability of T24 and 5673 cells after luteolin exposure for 48 h. B, C, Apoptosis was detected with phycoerythrin (PE), annexin V and 7-aminoactinomycin D (7-AAD) by flow cytometry. D, E, Cell-cycle assays were performed with propidium iodide (PI) staining and flow cytometry. Mean ± SD, **$P < 0.01$, ***$P < 0.001$ statistically significant compared with control group. F, Protein levels were detected by western blot analysis. G, Protein levels in RT4, a p53 wild-type human bladder cancer cell line, exposed to 10 μmol/L luteolin for 48 h were detected by western blot analysis. (H) The p21 protein was slightly induced by luteolin exposure for 48 h in RT4 cells with silenced TP53 by using small siRNA
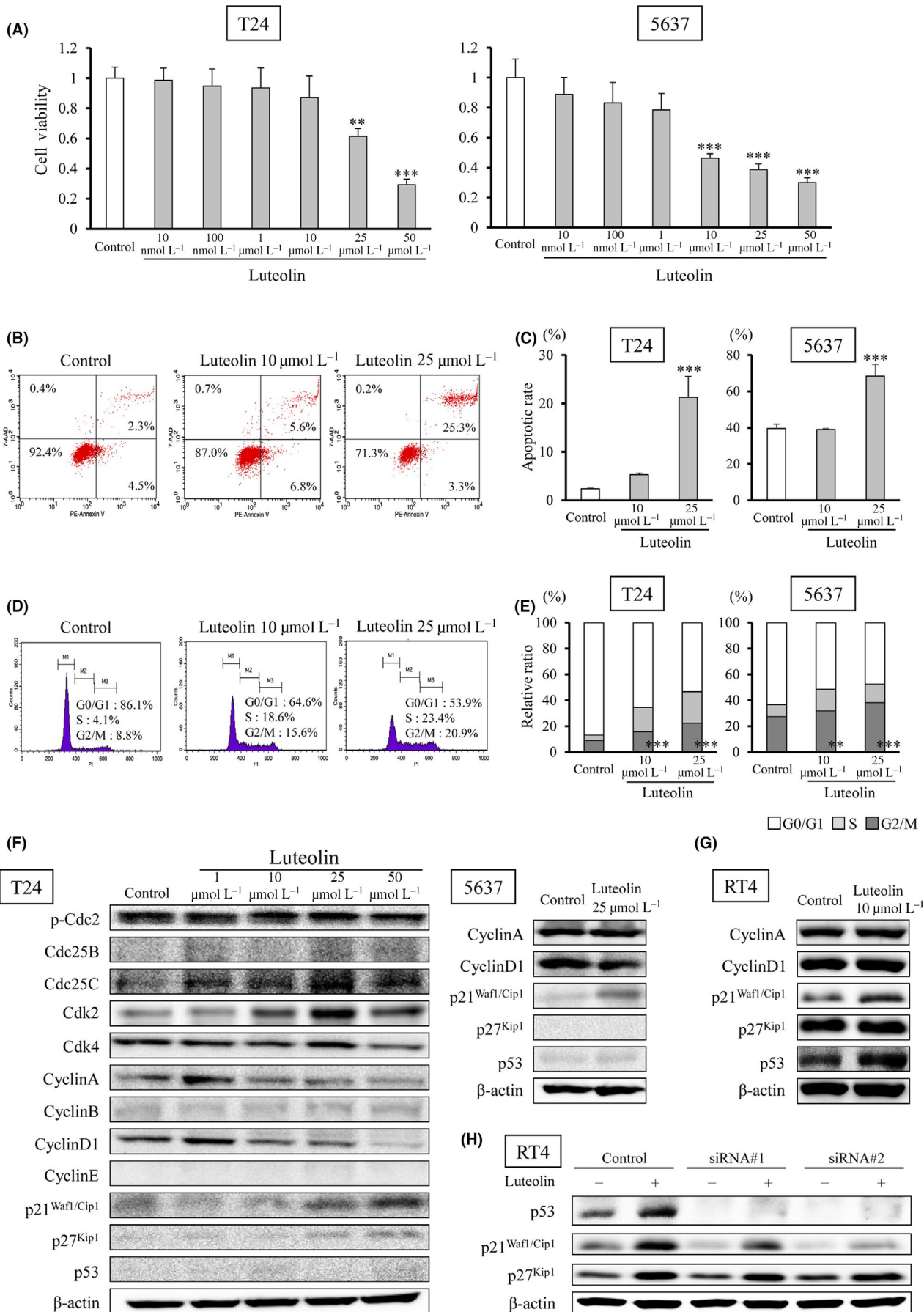
3.2 | Luteolin inhibits the mechanistic target of rapamycin pathway in bladder cancer

The mTOR regulates cell growth, proliferation, metabolism and autophagy. S6K is a major substrate of the mTOR kinase. The activity of S6K1, an isoform of S6K, is controlled with phosphorylation by mTOR, with the position of Thr389 being the most critical site of phosphorylation for kinase activity. S6 is a substrate of S6K regulated by phosphorylation and is involved in cell-cycle progression, ribosomal proteins, and elongation factors necessary for translation.[14,28,29]

Western blot analysis showed that levels of phospho(p)-Akt, phospho(p)-p70S6K and phospho(p)-S6 in bladder cancer cell lines were decreased by luteolin in a dose-dependent manner (Figure 2A,B). These effects were obtained 12 and 24 hours after exposure to luteolin (Figure 2C). We then compared the effect of luteolin to the mTOR inhibitor, Torin1. The inhibition of mTOR significantly reduced the survival rate at a concentration of more than 10 nmol/L,
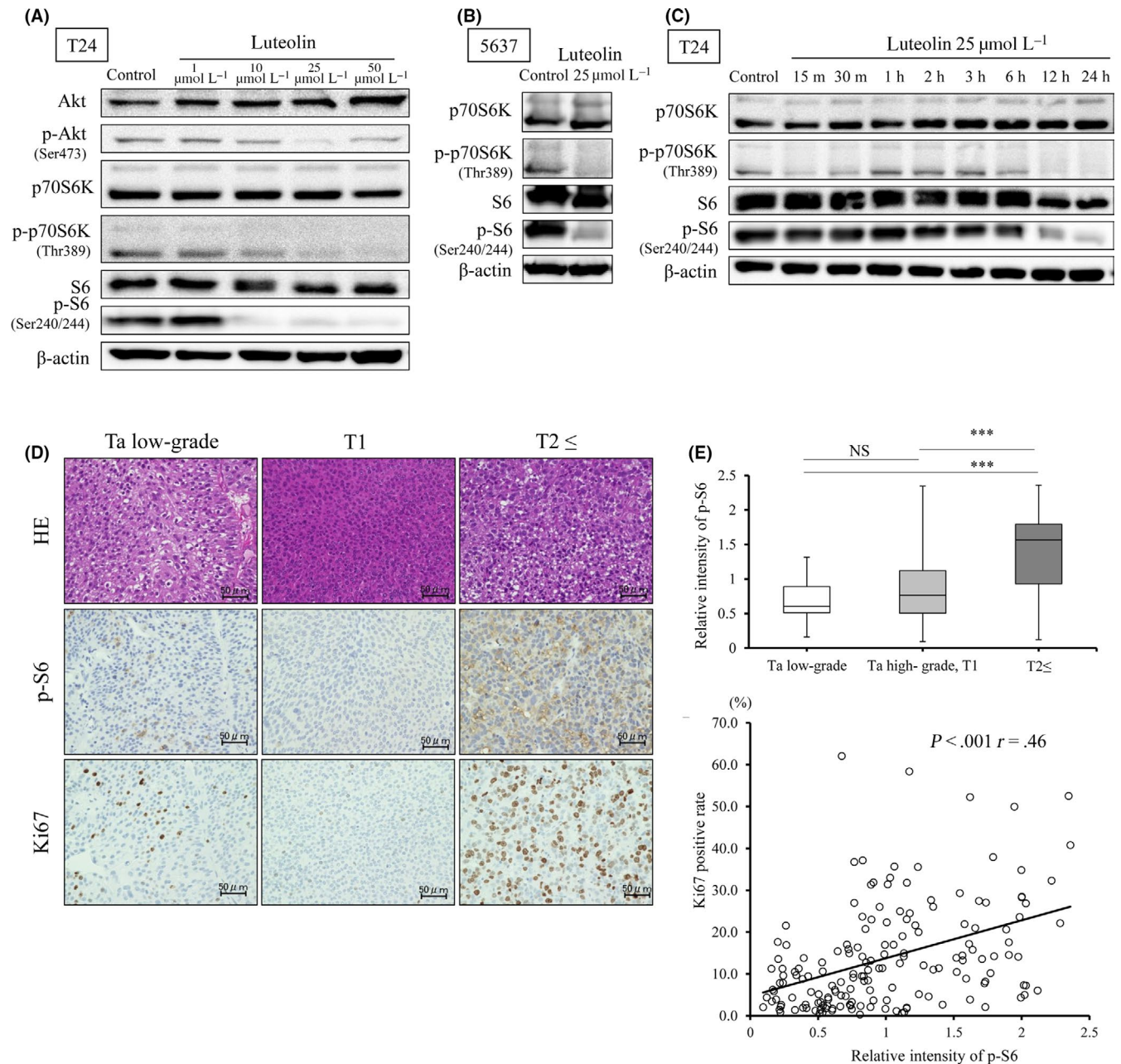

FIGURE 2 Luteolin inhibits the mechanistic target of rapamycin (mTOR) pathway in human bladder cancer. A-C, Western blot analysis of mTOR substrates and upstream signals in T24 (A) and 5637 (B) cells treated with luteolin for 48 h; mTOR substrates in T24 cells treated with luteolin over time (C). D, E, H&E staining and immunohistochemistry of phospho(p)-S6 and Ki67 were evaluated in 166 specimens from bladder cancer patients. Mean ± SD, ***P < 0.001. F, The correlation between p-S6 and Ki67 was analyzed by Spearman's rank correlation coefficient

and induced G1/S arrest and apoptosis in T24 cells (Figure S2A,C-F). Western blot analysis indicated that Torin1 treatment of T24 cells did not induce p21 expression, in contrast to luteolin (Figure S2B). These results suggest that the anti–tumor effect of luteolin was not phenocopied by an mTOR inhibitor and was affected by p21 in bladder cancer. (Figure S2A-D). Next, we evaluated the role of the mTOR pathway in patients with bladder cancer by analyzing the immunohistochemistry of p-S6 and Ki67. Although no statistical differences were found in the relative intensity of p-S6 between pTa low-grade and T1 plus Ta high-grade tumors, significant differences were found between more than T2 and pTa low-grade or T1 plus Ta high-grade tumors ($P < 0.001$, respectively; Figure 2D,E). A statistical correlation between the Ki67-labeling index and the relative intensity of p-S6 was evident ($P < 0.001$, $r = 0.46$; Figure 2F). These results indicate that mTOR activity may be related to cell proliferation in bladder cancer.

3.3 | The upregulation of TRX1 by luteolin suppresses cell proliferation in bladder cancer cells

We next evaluated whether luteolin affected the TRX1 level or the relationship between mTOR and TRX1. Intracellular ROS decreased and TRX1 increased in a concentration-dependent manner in luteolin-treated T24 cells (Figure 3A,B). To explore whether the suppressive effect of luteolin on cell viability can be attributed to TRX1 upregulation and whether TRX1 is associated with the mTOR pathway, we treated cells with the TRX1 inhibitor, PX-12.[11] PX-12 decreased T24 cell proliferation in a dose-dependent manner. This suggests that an imbalance in oxidative stress occurred that adversely affected cell viability (Figure 3C). T24 cells were harvested after 48-hour exposure to luteolin, followed by another 48-hour exposure to luteolin, DMSO control or 2 μmol/L PX-12 (nearly 40% decreased cell proliferation). Cells treated with luteolin followed by DMSO recovered from the decrease in cell survival induced by luteolin ($P < 0.001$; Figure 3D). PX-12 treatment also led to an increase in cell viability, despite the growth-suppressive concentration (Figure 3D). This indicates that TRX1 played a role in the inhibition of ROS production and cell proliferation in bladder cancer cells. Western blot analysis revealed that levels of p-p70S6K and p-S6 recovered with PX-12 treatment after luteolin-induced mTOR suppression quicker than those after DMSO treatment (exposure post–3-hour to PX-12 vs 12-24-hour to DMSO; Figure 3E). We further analyzed TRX1 expression and also prognosis by using a TCGA dataset of 338 patients with bladder cancer. Figure 3F,G shows no difference in the TRX1 level between normal and cancer tissues, and between low-grade and high-grade tumors. Furthermore, a significant difference in overall survival between high and low TRX1 expression groups was not observed (Figure 3H). These data indicate that TRX1 is not necessarily a negative prognostic factor in bladder cancer, unlike for other cancers,[9-11] and luteolin prevents the accumulation of intracellular ROS levels and mTOR signaling by upregulating the TRX1 level in bladder cancer.

3.4 | Anti–tumor effect of luteolin in a subcutaneous BC31 xenograft model

We next examined the anti–tumor effect of dietary luteolin in a subcutaneously transplanted BC31 xenograft model. Of 24 mice, the tumors of 10 out of 12 mice in the control group and 9 out of 12 mice in the luteolin 100 ppm group were successfully engrafted; and these 19 mice were subsequently used for analyzing the effect of luteolin. Significant differences in the amount of dietary intake, and body and organ weights between the two groups were not noted (Figure S3A-C). Histological analyses revealed that no toxic effect was induced by luteolin. The tumor volumes of mice of the luteolin 100 ppm group were significantly smaller than those of the control group of mice ($P < 0.05$; Figure 4A,B). Ki67-labeling index was significantly decreased and rates of TUNEL-positive cells were significantly increased by luteolin ($P < 0.001$ for both; Figure 4C). These results suggest that luteolin inhibited proliferation and induced apoptosis in bladder cancer cell xenografts (Figure 4C). The percentage of p21-positive cells was significantly higher ($P < 0.01$) and p-S6 intensity was significantly lower ($P < 0.001$) in the luteolin 100 ppm group compared to the control group, which was consistent with in vitro results (Figure 4C).

3.5 | Luteolin metabolites decrease mechanistic target of rapamycin signaling and cell proliferation in an N-butyl-N-(4-hydroxybutyl) nitrosamine-induced rat bladder cancer model

Finally, we investigated the anti–tumor effect of the oral intake of luteolin using a BBN-induced rat bladder cancer model. A rat in the 100-ppm group died because of bladder cancer without metastasis or hydronephrosis the day before it was due to be killed. Significant differences in the amount of BBN water, dietary intake, and body and organ weights among the three groups were not observed (Figure S4A-D). No histological change was observed in livers and kidneys.

All rats developed superficial bladder cancer without invasion. DNA sequencing analysis revealed that point mutations of *p53* gene were observed in rat bladder cancers (Table S3). Mutations in codon 195 (GTG → ATG) and codon 251 (ACC → ATC) were similar to those reported in a previous study.[26] Bladder weight and tumor dimension tended to be reduced by luteolin treatment (Figure 5A-C). Immunohistochemical analyses revealed a significantly decreased Ki67-labeling index ($P < 0.01$) and p-S6 level ($P < 0.001$) in the high-dose luteolin group, but differences in positive rates of TUNEL and p21 staining were not observed (Figure 5D). We further analyzed any change in squamous differentiation, which relates to worse recurrence and progression rates[30] with luteolin, because we previously found that the oxidative stress-regulated gene glutathione peroxidase 2 (*GPX2*) was upregulated in several carcinomas, including UC,[22,27,31,32] and promoted squamous differentiation.[22] Moreover, we recently found that luteolin downregulated GPX2 in the rat prostate tumor and in a human prostate cancer cell line.[33] The frequency of squamous differentiation in the
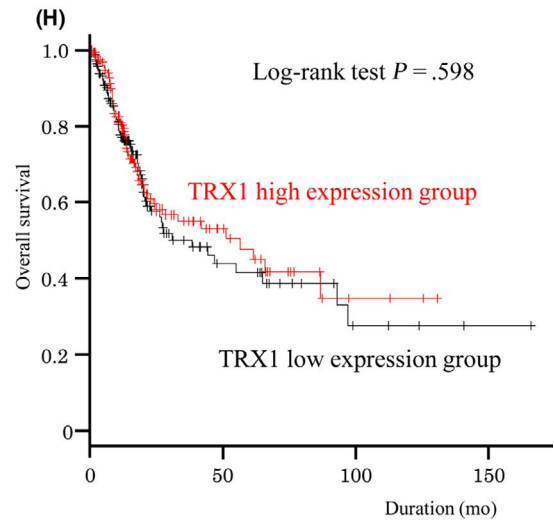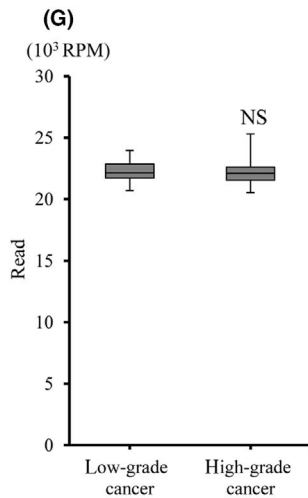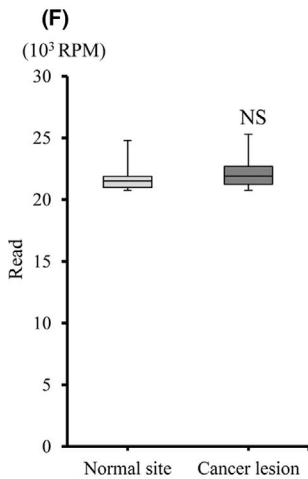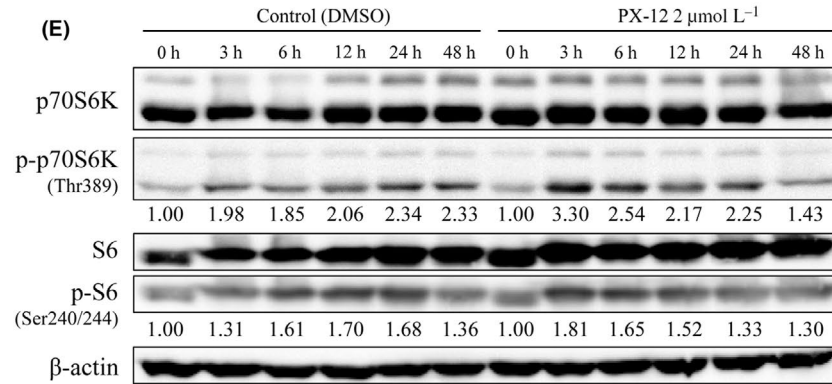
(A) Relative ROS production — Control, Luteolin 1 μmol L⁻¹, 10 μmol L⁻¹, 25 μmol L⁻¹ (**), 50 μmol L⁻¹ (***)

(B) Relative thioredoxin level — Control, Luteolin 1 μmol L⁻¹, 10 μmol L⁻¹ (**), 25 μmol L⁻¹ (***), 50 μmol L⁻¹ (***)

(C) Cell viability — Control, PX-12 100 nmol L⁻¹, 1 μmol L⁻¹, 1.5 μmol L⁻¹ (*), 2 μmol L⁻¹ (***), 2.5 μmol L⁻¹ (***), 3 μmol L⁻¹ (***)

(D) Cell viability — Control, Luteolin 25 μmol L⁻¹ (***), PX-12 2 μmol L⁻¹; NS

(E) Western blot — Control (DMSO) and PX-12 2 μmol L⁻¹ at 0 h, 3 h, 6 h, 12 h, 24 h, 48 h

p70S6K

p-p70S6K (Thr389): Control 1.00, 1.98, 1.85, 2.06, 2.34, 2.33; PX-12 1.00, 3.30, 2.54, 2.17, 2.25, 1.43

S6

p-S6 (Ser240/244): Control 1.00, 1.31, 1.61, 1.70, 1.68, 1.36; PX-12 1.00, 1.81, 1.65, 1.52, 1.33, 1.30

β-actin

(F) (10³ RPM) Read — Normal site, Cancer lesion; NS

(G) (10³ RPM) Read — Low-grade cancer, High-grade cancer; NS

(H) Overall survival vs Duration (mo); Log-rank test P = .598; TRX1 high expression group (red); TRX1 low expression group (black)
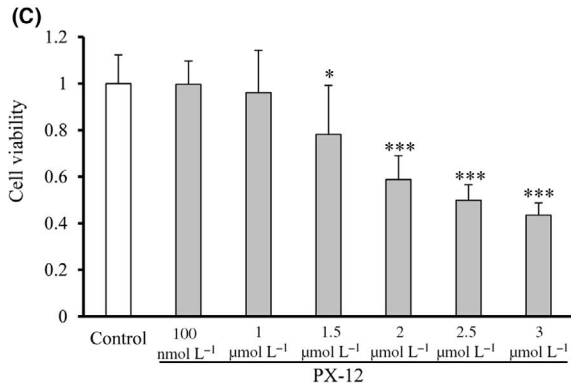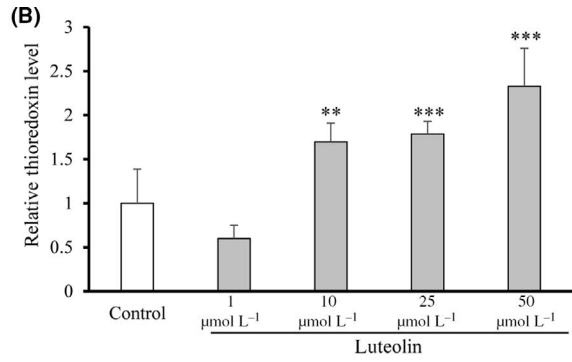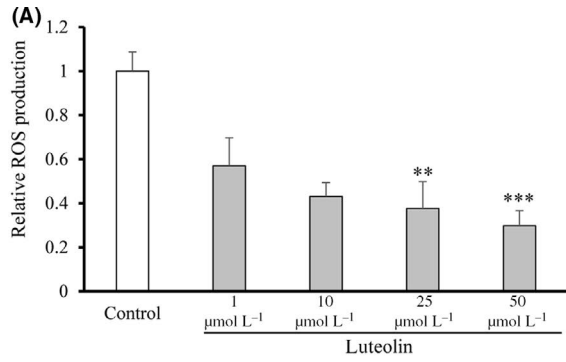
FIGURE 3 Luteolin decreases intracellular reactive oxygen species (ROS) by upregulating TRX1 in human bladder cancer cells. A, B, ROS (A) and TRX1 (B) levels in T24 cells with 48-h exposure to luteolin were evaluated by DCFH-DA and thioredoxin assays, respectively. C, Cell viability assay of T24 treated with TRX1 inhibitor, PX12, for 48 h. Mean ± SD, *$P < 0.05$, ***$P < 0.001$. D, Effect of TRX1 on decreased cell viability by luteolin. T24 cells were treated with PX-12 for 48 h after increasing the activity of TRX1 with a 48-h exposure of cells to luteolin. E, Western blot analysis over time of mTOR substrates after 48-h exposure to luteolin following 48-h treatment of T24 cells with PX-12. F, G, TRX1 mRNA expression in normal and tumor tissues (n = 19, respectively), and in low-grade and high-grade tumors (n = 20, 318, respectively) from The Cancer Genome Atlas (TCGA) bladder cancer dataset. Mean ± SD. H, Kaplan–Meier curves of high and low expression TRX1 groups from a TCGA bladder cancer dataset (n = 335); cancers were divided into two groups according to the median TRX1 expression. The *P*-value was obtained by log-rank test
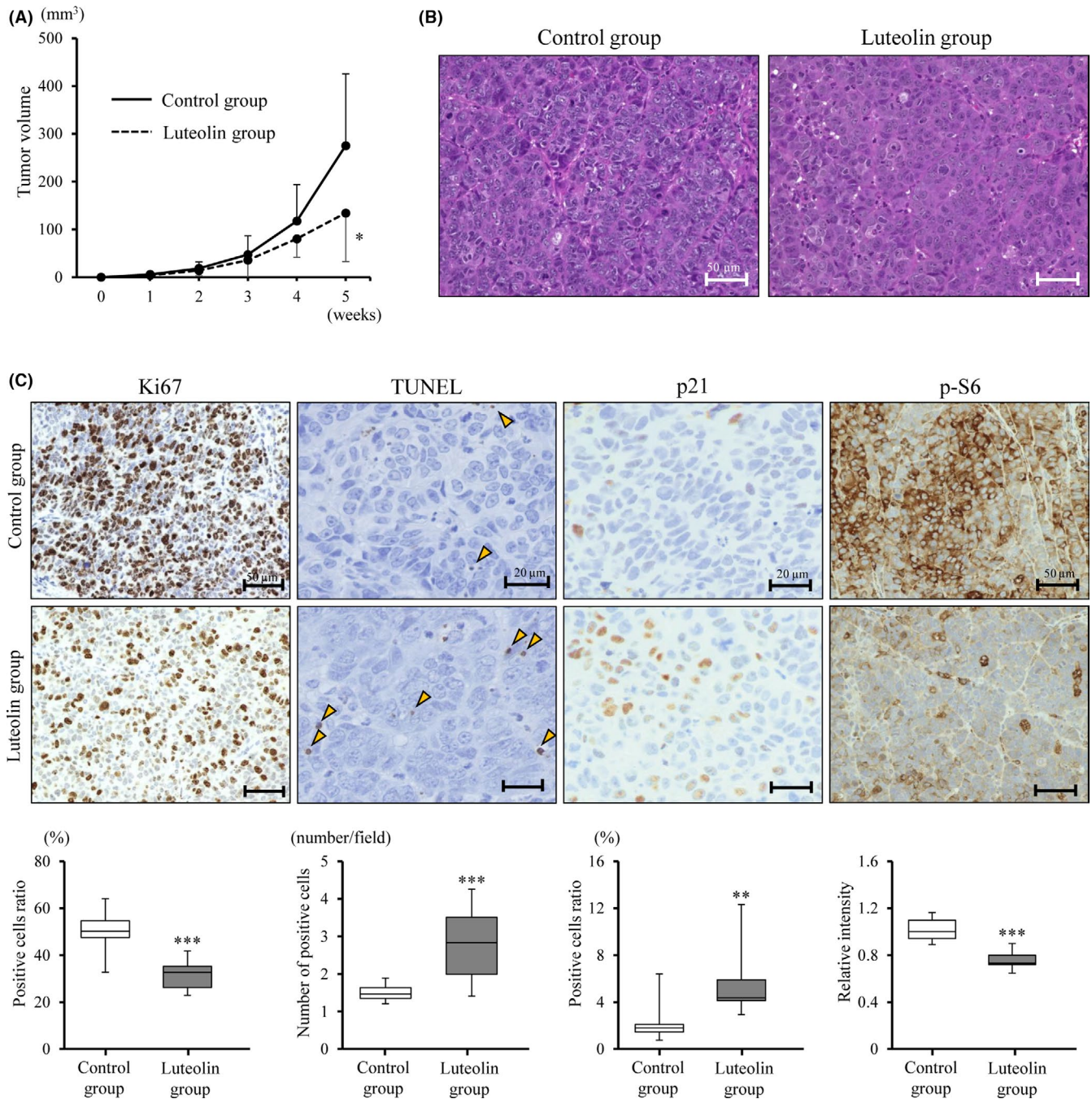

FIGURE 4 Luteolin attenuates rat bladder xenograft tumor growth through inactivation of mechanistic target of rapamycin (mTOR) and upregulation of p21. A, Tumor volume of BC31 xenografts in nude mice received a control diet or a diet with luteolin. B, H&E staining of BC31 tumors. C, Immunohistochemistry of Ki67, p21 and phospho(p)-S6 in TUNEL assays of tumors. The bottom bar charts show quantitative levels. Mean ± SD, n = 10 (control), n = 9 (luteolin), *$P < 0.05$, **$P < 0.01$ and ***$P < 0.001$ are statistically significant compared with the control group
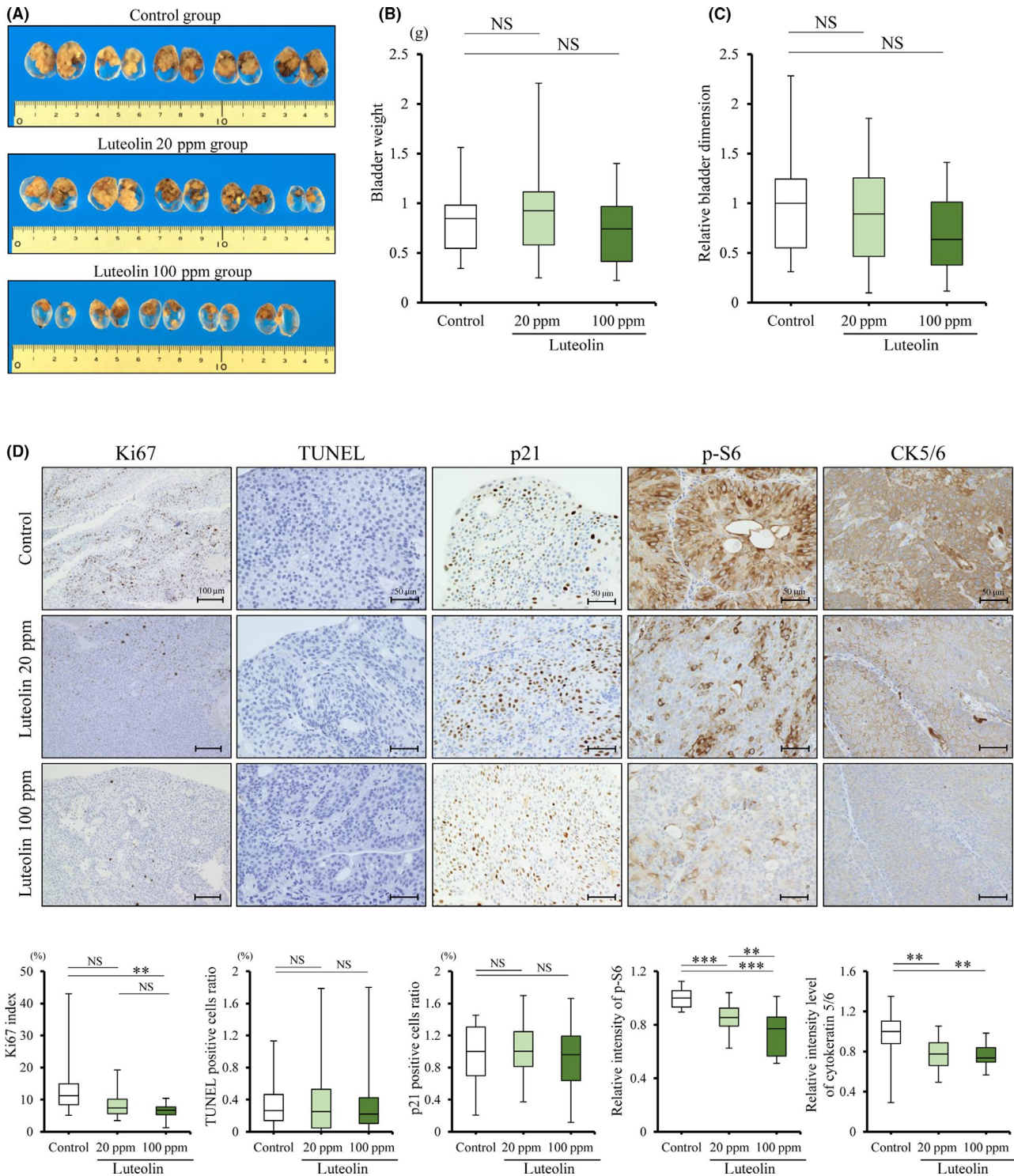
FIGURE 5 Luteolin decreases proliferation and squamous differentiation through inactivation of mechanistic target of rapamycin (mTOR) in N-butyl-N-(4-hydroxybutyl) nitrosamine (BBN)-induced rat bladder cancer model. A, Representative macroscopic findings of rat bladder cancer from control and luteolin (Lut; 20, 100 ppm)-treated groups in a bladder cancer model induced by BBN. B, C Bladder weights (B) and relative tumor dimensions (C) after each treatment. D, Immunohistochemistry of Ki67, p21, phospho(p)-S6 and cytokeratin 5/6 (CK5/6) and TUNEL assay in tumors. The bottom charts show quantitative levels. Mean ± SD, n = 20 per group, **$P < 0.01$, ***$P < 0.001$ statistically significant compared with control group. E, H&E staining of a case of urothelial carcinoma (UC) with squamous differentiation. F, Number of cases of UC with squamous differentiation in each group. P-values were obtained by Fisher's exact test. Mean ± SD, *$P < 0.05$ statistically significant compared with control group. G, Immunohistochemistry of glutathione peroxidase 2 (GPX2) in tumors in bladder cancer models induced by BBN. H, Relative intensity of GPX2 in the three groups (control, 20 ppm, and 100 ppm luteolin). Mean ± SD, n = 20 per group, **$P < 0.01$, ***$P < 0.001$ statistically significant compared with control group. I, Relative intensity of GPX2 in urothelial carcinoma (UC) with and without squamous differentiation (n = 36, n = 24, respectively). Mean ± SD, ****$P < 0.0001$ statistically significant

(E)
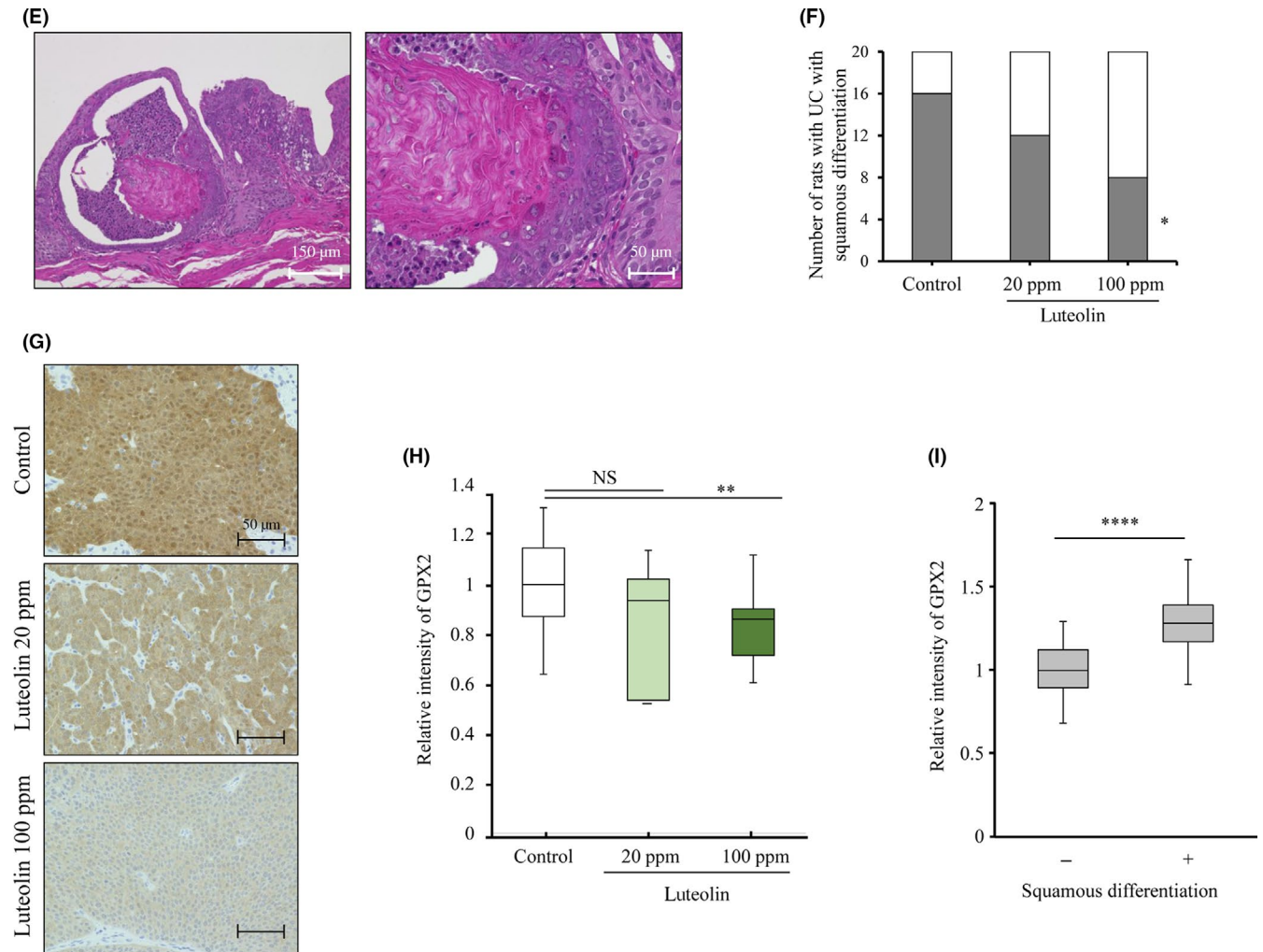

(F)

(G)

(H)

(I)

FIGURE 5 (Continued)

tumors was significantly decreased in the luteolin-treated groups ($P < 0.05$; Figure 5E,5). Consistent with this result, the level of CK5/6, a marker of squamous differentiation,[30,34] was decreased by luteolin treatment ($P < 0.01$; Figure 5D,E). Immunohistochemistry revealed that the expression of GPX2 was induced in bladder cancer with squamous differentiation, compared to pure UC, and was significantly reduced by luteolin in rat BBN-induced bladder cancer ($P < 0.01$; Figure 5G,H). Moreover, the expression level of GPX2 and the incidence of squamous differentiation were significantly correlated in the model ($P < 0.001$; Figure 5I). GPX2 expression was shown in RT4 and BC31 cells but not in T24 and 5637 cells, and was not affected by luteolin treatment in vitro (Figure S5). These results indicate that luteolin reduces squamous differentiation through the suppression of GPX2 in rat bladder cancer in vivo.

Next, we analyzed the metabolism of luteolin and whether it is involved in the anti–cancer effect. Previous reports described the oral administration of luteolin-aglycone or glucoside and their conjugation to glucuronide in rats occurring mainly in plasma and tissues.[35,36] Consistent with this, luteolin-aglycone and glucoside were not detected in plasma. Instead, concentrations of luteolin-3′-glucuronide in plasma (1.66 ± 1.30 ng/mL) and urine (25.1 ± 18.5 ng/mL),

respectively, were significantly increased after luteolin treatment (Figure 6A). Concentrations of luteolin-3′-glucuronide showed a mild correlation between urine and plasma ($r = 0.25$, $P = 0.20$; Figure 6B).

The luteolin-3′-glucuronide concentration in urine ($r = -0.41$, $P = 0.03$), as well as that in plasma ($r = -0.31$, $P = 0.11$), was significantly correlated with the Ki67-labeling index of the tumors (Figure 6C), even though it did not correlate with tumor dimension (Figure 6D). Moreover, the relative p-S6 intensity of the tumors and luteolin-3′-glucuronide concentration in plasma, as well as that in urine, showed a strong correlation ($r = -0.60$, $P < 0.001$ and $r = -0.62$, $P < 0.001$, respectively; Figure 6E). With respect to the preventive effect of luteolin on squamous differentiation, luteolin-3′-glucuronide concentrations in plasma were significantly correlated with a lack of squamous differentiation and low GPX2 intensity ($P < 0.01$; Figure 6F, $P < 0.01$; Figure 6G).

4 | DISCUSSION

Luteolin inhibits cell growth by regulating the cell cycle in several cancers.[6-8] A member of the Cip/Kip family, p21 shares an N-terminal domain that binds cyclins and cyclin-dependent kinases (CDK).[37] In
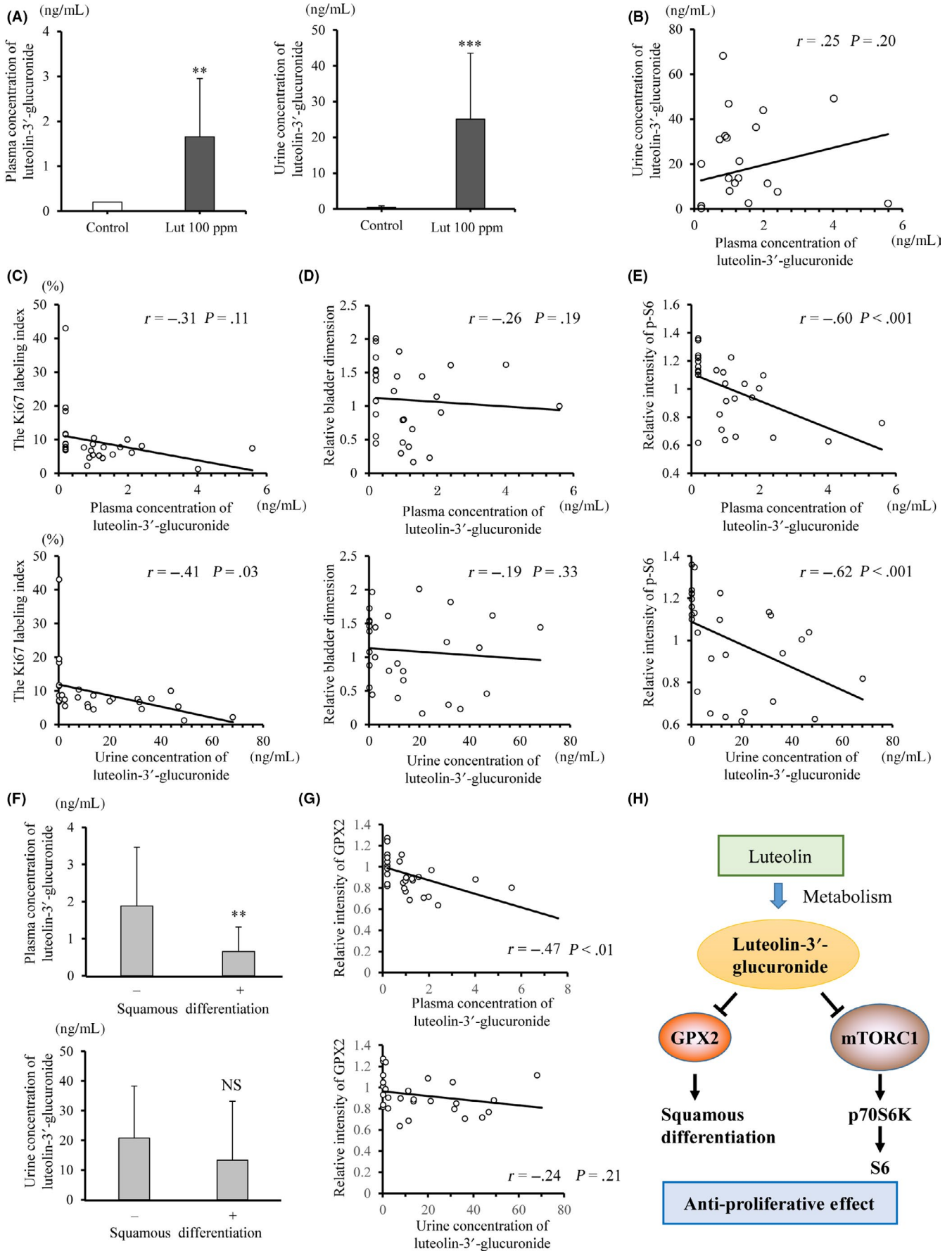
bladder cancer, decreased p21 expression was associated with reduced survival and increased recurrence after radical cystectomy, suggesting that p21 has tumor-suppressive roles in bladder cancer.[38-40] In the present study, luteolin upregulated p21 and induced G2/M arrest in human bladder cancer cells. The p21 protein is well-known as a regulator of G1/S; however, G1 and G2 arrest are induced by p21 through the inhibition of cyclin/CDK2 complexes.[41] This suggests that p21 affects multiple phases of the cell cycle, depending on the cellular context.

When a "p21-positive bladder tumor" was defined as more than 10% of the bladder cancer cells were expressing p21, the incidence of p21-positive bladder tumor cases was 33%-64%.[38-40] As similarly defined in a BBN-induced rat bladder cancer model in the present study, more than 98% of rats (58/59 rats) were p21-positive, with p21-positive rates in each rat being 27.8 ± 10.5%. The higher expression of p21 in the rat may have led to an insignificant change in p21 by luteolin treatment in the present rat BBN bladder cancer model.

Both in vitro and in vivo studies showed that luteolin inhibited the mTOR pathway in bladder cancer. Reduced levels of p-S6 downregulated mTOR in human bladder cancer specimens and this was significantly correlated with disease progression and disease-specific survival.[42,43] The present study demonstrates that p-S6 was upregulated during stage progression and was correlated with the Ki67-labeling index in human bladder cancers. This suggests that p-S6 may reflect not only the prognosis but also the ability of tumors to proliferate or invade in bladder cancer.

We focused on TRX1 function in bladder cancer because it is an anti–oxidative gene that is involved in mTOR signaling. Luteolin upregulated TRX1 and downregulated mTOR signaling in human bladder cancer, while an TRX1 inhibitor induced recovery from mTOR activation. These results suggest TRX1 is a tumor-suppressive gene in bladder cancer. A significant difference between TRX1 expression and prognosis in bladder cancer cases is not found, meaning that TRX1 may be an inducible suppressor of proliferation by reacting with an anti–cancer agent such as luteolin. Indeed, Yokomizo et al indicated that TRX1 levels are associated with drug sensitivity in T24 cells.[44] However, further study is needed to elucidate the function of TRX1 as an anti–cancer agent in bladder cancer.

We investigated the anti–tumor activity of orally administered luteolin using a rat BC31 xenograft and a BBN-induced bladder carcinogenesis model. The Ki67-labeling index and mTOR activation represented by p-S6 expression were significantly decreased by dietary luteolin consumption in both rodent models. However, significant tumor suppression was detected only in the BC31 xenograft model. In the BBN-induced rat bladder cancer model, the incidence and size of tumors have been reported to be

in accordance with concentration, duration and post–duration of BBN intake.[45,46] The present study set a BBN intake for 10 weeks followed by 20 weeks of luteolin administration. This induced bigger tumors and individual variability in all treatment groups due to the difficulty in the analysis of preneoplastic foci-like hyperplasia. This is one reason why tumors in luteolin-treated animals were not significantly different from those of controls. In line with a decreased Ki67-labeling index and mTOR activity, luteolin may also have a suppressive role in BBN-induced rat bladder carcinogenesis.

We further determined the relationship between level of lueolin in the body and a suppressive role in bladder carcinogenesis. Luteolin-aglycone is absorbed directly into the intestine, but luteolin-7-glucoside is absorbed after hydrolysis to form luteolin-aglycone. The most abundant metabolite of luteolin is luteolin-3′-glucuronide in rats and occurs because luteolin-aglycone and glucoside are conjugated to glucuronide in the small intestine, liver and kidneys by phase II enzymes.[35] In comparison, the major metabolite of luteolin in human plasma is luteolin-3′-sulfate, which is believed to be converted by phenol sulfotransferase in the intestine.[35,47] The half maximal concentration of luteolin-3′-glucuronide in rat plasma after the oral administration of luteolin-aglycone occurred at 12 hours, while that of luteolin-3′-sulfate in humans occurred at approximately 6 hours. This difference is explained by the enterohepatic recycling of glucuronide.[48] Flavonoid glucuronide is excreted into feces and urine, while flavonoid sulfates are mainly excreted in urine.[35,36]

In this study, the amount of daily feed intake was 12.6 g/d/rat in the BBN model (Figure S3B), which was converted into luteolin-aglycone at 1.26 mg per day (3.5 mg/kg) in the 100-ppm luteolin group. The plasma and urine concentrations of luteolin-3′-glucuronide were 1.66 ± 1.30 and 25.1 ± 18.5 ng/mL, respectively, in rats treated with 100 ppm luteolin. This were equivalent to 3.6 ± 2.8 μmol/L and 54.3 ± 40.0 μmol/L, respectively, in vitro. These were almost the same concentrations as found in in vitro experiments, after 10-25 μmol/L luteolin treatment, in this study.

Several studies on the relationship between concentrations of luteolin metabolites and anti–inflammatory effects have been reported.[30,34-36] However, few studies have focused on the concentrations of luteolin metabolites and their anti–cancer effects in vivo. The major findings of the present in vivo study were as follows (Figure 6H). First, both plasma and urine concentrations of luteolin-3′-glucuronide were significantly correlated with decreased Ki67-labeling indices and p-S6. Second, the plasma level of luteolin-3′-glucuronide is related to the suppression of squamous differentiation of bladder tumors, which led to a poor prognosis in human bladder cancer.[30,34] Our study provides new insight into how luteolin alleviates not only proliferation

but also squamous differentiation of bladder cancer. Therefore, luteolin may have potential as an anti–cancer agent for bladder cancer, although further studies are warranted.

ACKNOWLEDGMENTS

DISCLOSURE

The authors have no conflict of interest to declare.

ORCID

Taku Naiki 🆔 https://orcid.org/0000-0002-7638-6048
Aya Naiki-Ito 🆔 https://orcid.org/0000-0003-0828-2033
Shugo Suzuki 🆔 https://orcid.org/0000-0001-8938-9670
Takahiro Yasui 🆔 https://orcid.org/0000-0003-2197-2477
Satoru Takahashi 🆔 https://orcid.org/0000-0002-8139-8158

REFERENCES

1. Bray F, Ferlay J, Soerjomataram I, Siegel RL, Torre LA, Jemal A. Global cancer statistics 2018: GLOBOCAN estimates of incidence and mortality worldwide for 36 cancers in 185 countries. *CA Cancer J Clin*. 2018;68:394-424.
2. Bellmunt J, de Wit R, Vaughn DJ, et al. Pembrolizumab as second-line therapy for advanced urothelial carcinoma. *N Engl J Med*. 2017;376:1015-1026.
3. Cumberbatch MG, Rota M, Catto JW, La Vecchia C. The role of tobacco smoke in bladder and kidney carcinogenesis: a comparison of exposures and meta-analysis of incidence and mortality risks. *Eur Urol*. 2016;70:458-466.
4. Mena S, Ortega A, Estrela JM. Oxidative stress in environmental-induced carcinogenesis. *Mutat Res*. 2009;674:36-44.
5. Schieber M, Chandel NS. ROS function in redox signaling and oxidative stress. *Curr Biol*. 2014;24:R453-R462.
6. Imran M, Rauf A, Abu-Izneid T, et al. Luteolin, a flavonoid, as an anticancer agent: A review. *Biomed Pharmacother*. 2019;112:108612.
7. Pandurangan AK, Esa NM. Luteolin, a bioflavonoid inhibits colorectal cancer through modulation of multiple signaling pathways: a review. *Asian Pac J Cancer Prev*. 2014;15:5501-5508.
8. Sagawa H, Naiki-Ito A, Kato H, et al. Connexin 32 and luteolin play protective roles in non–alcoholic steatohepatitis development and its related hepatocarcinogenesis in rats. *Carcinogenesis*. 2015;36:1539-1549.
9. Kim SJ, Miyoshi Y, Taguchi T, et al. High thioredoxin expression is associated with resistance to docetaxel in primary breast cancer. *Clin Cancer Res*. 2005;11:8425-8430.
10. Noike T, Miwa S, Soeda J, Kobayashi A, Miyagawa S. Increased expression of thioredoxin-1, vascular endothelial growth factor, and redox factor-1 is associated with poor prognosis in patients with liver metastasis from colorectal cancer. *Hum Pathol*. 2008;39: 201-208.
11. Samaranayake GJ, Troccoli CI, Huynh M, et al. Thioredoxin-1 protects against androgen receptor-induced redox vulnerability in castration-resistant prostate cancer. *Nat Commun*. 2017;8:1204.
12. Kaimul AM, Nakamura H, Masutani H, Yodoi J. Thioredoxin and thioredoxin-binding protein-2 in cancer and metabolic syndrome. *Free Radic Biol Med*. 2007;43:861-868.
13. Gorrini C, Harris IS, Mak TW. Modulation of oxidative stress as an anticancer strategy. *Nat Rev Drug Discov*. 2013;12:931-947.
14. Bjornsti MA, Houghton PJ. The TOR pathway: a target for cancer therapy. *Nat Rev Cancer*. 2004;4:335-348.
15. Chiong E, Lee IL, Dadbin A, et al. Effects of mTOR inhibitor everolimus (RAD001) on bladder cancer cells. *Clin Cancer Res*. 2011;17:2863-2873.
16. Oliveira PA, Arantes-Rodrigues R, Sousa-Diniz C, et al. The effects of sirolimus on urothelial lesions chemically induced in ICR mice by BBN. *Anticancer Res*. 2009;29:3221-3226.
17. Milowsky MI, Iyer G, Regazzi AM, et al. Phase II study of everolimus in metastatic urothelial cancer. *BJU Int*. 2013;112:462-470.
18. Seront E, Rottey S, Filleul B, et al. Phase II study of dual phosphoinositol-3-kinase (PI3K) and mammalian target of rapamycin (mTOR) inhibitor BEZ235 in patients with locally advanced or metastatic transitional cell carcinoma. *BJU Int*. 2016;118:408-415.
19. Yoshida S, Hong S, Suzuki T, et al. Redox regulates mammalian target of rapamycin complex 1 (mTORC1) activity by modulating the TSC1/TSC2-Rheb GTPase pathway. *J Biol Chem*. 2011;286:32651-32660.
20. Sarbassov DD, Sabatini DM. Redox regulation of the nutrient-sensitive raptor-mTOR pathway and complex. *J Biol Chem*. 2005;280:39505-39509.
21. Oka SI, Hirata T, Suzuki W, et al. Thioredoxin-1 maintains mechanistic target of rapamycin (mTOR) function during oxidative stress in cardiomyocytes. *J Biol Chem*. 2017;292:18988-19000.
22. Naiki T, Naiki-Ito A, Iida K, et al. GPX2 promotes development of bladder cancer with squamous cell differentiation through the control of apoptosis. *Oncotarget*. 2018;9:15847-15859.
23. Ito A, Asamoto M, Hokaiwado N, Takahashi S, Shirai T. Tbx3 expression is related to apoptosis and cell proliferation in rat bladder both hyperplastic epithelial cells and carcinoma cells. *Cancer Lett*. 2005;219:105-112.
24. Ito A, Asamoto M, Hokaiwado N, Shirai T. Regulation of cell proliferation by induction of p21/WAF1 in rat bladder carcinoma cells using the Cre–loxP system. *Cancer Lett*. 2003;193:183-188.
25. Frazier KS, Seely JC, Hard GC, et al. Proliferative and nonproliferative lesions of the rat and mouse urinary system. *Toxicol Pathol*. 2012;40:14S-86S.
26. Masui T, Dong Y, Yamamoto S, et al. p53 mutations in transitional cell carcinomas of the urinary bladder in rats treated with N-butyl-N-(4-hydroxybutyl)-nitrosamine. *Cancer Lett*. 1996;105:105-112.
27. Naiki-Ito A, Asamoto M, Hokaiwado N, et al. Gpx2 is an overexpressed gene in rat breast cancers induced by three different chemical carcinogens. *Cancer Res*. 2007;67:11353-11358.
28. Hay N, Sonenberg N. Upstream and downstream of mTOR. *Genes Dev*. 2004;18:1926-1945.
29. Pullen N, Thomas G. The modular phosphorylation and activation of p70s6k. *FEBS Lett*. 1997;410:78-82.
30. Erdemir F, Tunc M, Ozcan F, et al. The effect of squamous and/or glandular differentiation on recurrence, progression and survival in urothelial carcinoma of bladder. *Int Urol Nephrol*. 2007;39:803-807.
31. Naiki T, Naiki-Ito A, Asamoto M, et al. GPX2 overexpression is involved in cell proliferation and prognosis of castration-resistant prostate cancer. *Carcinogenesis*. 2014;35:1962-1967.
32. Suzuki S, Pitchakarn P, Ogawa K, et al. Expression of glutathione peroxidase 2 is associated with not only early hepatocarcinogenesis but also late stage metastasis. *Toxicology*. 2013;311:115-123.
33. Naiki-Ito A, Naiki T, Kato H, et al. Recruitment of miR-8080 by luteolin inhibits androgen receptor splice variant 7 expression in castration-resistant prostate cancer. *Carcinogenesis*. 2019; in press.
34. Kim SP, Frank I, Cheville JC, et al. The impact of squamous and glandular differentiation on survival after radical cystectomy for urothelial carcinoma. *J Urol*. 2012;188:405-409.

35. Hayasaka N, Shimizu N, Komoda T, et al. Absorption and metabolism of luteolin in rats and humans in relation to in vitro anti–inflammatory effects. *J Agric Food Chem.* 2018;66:11320-11329.

36. Kure A, Nakagawa K, Kondo M, et al. Metabolic fate of luteolin in rats: its relationship to anti–inflammatory effect. *J Agric Food Chem.* 2016;64:4246-4254.

37. Besson A, Dowdy SF, Roberts JM. CDK inhibitors: cell cycle regulators and beyond. *Dev Cell.* 2008;14:159-169.

38. Chatterjee SJ, Datar R, Youssefzadeh D, et al. Combined effects of p53, p21, and pRb expression in the progression of bladder transitional cell carcinoma. *J Clin Oncol.* 2004;22:1007-1013.

39. Shariat SF, Tokunaga H, Zhou J, et al. p53, p21, pRB, and p16 expression predict clinical outcome in cystectomy with bladder cancer. *J Clin Oncol.* 2004;22:1014-1024.

40. Stein JP, Ginsberg DA, Grossfeld GD, et al. Effect of p21WAF1/CIP1 expression on tumor progression in bladder cancer. *J Natl Cancer Inst.* 1998;90:1072-1079.

41. Niculescu AB 3rd, Chen X, Smeets M, Hengst L, Prives C, Reed SI. Effects of p21(Cip1/Waf1) at both the G1/S and the G2/M cell cycle transitions: pRb is a critical determinant in blocking DNA replication and in preventing endoreduplication. *Mol Cell Biol.* 1998;18:629-643.

42. Park SJ, Lee TJ, Chang IH. Role of the mTOR pathway in the progression and recurrence of bladder cancer: an immunohistochemical tissue microarray study. *Korean J Urol.* 2011;52:466-473.

43. Schultz L, Albadine R, Hicks J, et al. Expression status and prognostic significance of mammalian target of rapamycin pathway members in urothelial carcinoma of urinary bladder after cystectomy. *Cancer.* 2010;116:5517-5526.

44. Yokomizo A, Ono M, Nanri H, et al. Cellular levels of thioredoxin associated with drug sensitivity to cisplatin, mitomycin C, doxorubicin, and etoposide. *Cancer Res.* 1995;55:4293-4296.

45. Osawa S, Terashima Y, Kimura G, Akimoto M. Antitumour effects of the angiogenesis inhibitor AGM-1470 on rat urinary bladder tumours induced by N-butyl-N-(4-hydroxybutyl) nitrosamine. *BJU Int.* 1999;83:123-128.

46. Ozono S, Babaya K, Sasaki K, et al. Rat urinary bladder carcinomas induced by N-butyl-N-(4-hydroxybutyl)-nitrosamine and N-methyl-N-nitrosourea. *Urol Res.* 1990;18:323-326.

47. Murota K, Terao J. Antioxidative flavonoid quercetin: implication of its intestinal absorption and metabolism. *Arch Biochem Biophys.* 2003;417:12-17.

48. Xia B, Zhou Q, Zheng Z, Ye L, Hu M, Liu Z. A novel local recycling mechanism that enhances enteric bioavailability of flavonoids and prolongs their residence time in the gut. *Mol Pharm.* 2012;9:3246-3258.

SUPPORTING INFORMATION

Additional supporting information may be found online in the Supporting Information section.